Preparation and Research on the Performance of PPV/PVP/Au Composite Nanofibers by Electrospinning

Eryun Yan[1], Guoqiang Xu[2], Shuhong Wang[2], Cheng Wang[2,*], Changlong Yang[1], Yang Xie[2], Lili Lv[2], Liang Ni[2], Tao Jing[3,*]

[1] College of Materials Science and Engineering, Qiqihar University, Qiqihar 161006, P.R. China
[2] Key Laboratory of Functional Inorganic Material Chemistry (Heilongjiang University), Ministry of Education, Harbin 150080, P.R. China
[3] College of Chemistry and Chemical Engineering, Qiqihar University, Qiqihar 161006, P.R. China;
Key Laboratory of Polymer Composition and Modification, College of Heilongjiang Province

Poly(phenylene vniylene)/polyvinylpyrrolidone/Au (PPV/PVP/Au) composite nanofibers with photoelectric properties were prepared by compositing Au nanoparticles (NPs) with PVP and PPV via electrospinning technique. The results of scanning electron microscopy (SEM) and transmission electron microscopy (TEM) showed that the composite nanofibers had uniform and continuous morphology and with the increase of Au content, the diameter of nanofibers decreased from 583 to 415 nm. Au NPs were face-centered cubic structure with an average diameter of 21 nm, and their existence had not affect the photoluminescence (PL) positions of PPV/PVP composites. The as-prepared PPV/PVP/Au composite nanofibers exhibited relatively high photoelectric intensity and they will have potential applications in photoelectric field.

1. INTRODUCTION

With the development of nanotechnology, a lot of new nanomaterials with superior performance have been discovered. Inorganic/organic composite nanomaterials are one of them, which possess both the advantages of the organic materials, such as flexibility and light weight, and the inorganic materials, such as heat and chemical resistances [1-4].

Among all the polymers, poly(phenylene vinylene) (PPV) possesses excellent photoluminescent (PL) [5, 6], electroluminescent (EL), photovoltaic (PV) and non-linear optical properties [7-9]. These properties have led to its broad applications, in such areas as light-emitting

diodes (LEDs) and flat panel displays. Therefore, PPV has become one of the most famous semiconducting polymers since 1990 [10]. Polyvinyl pyrrolidone (PVP) is a nonionic water-soluble polymer, and the carbonyl on the pyrrolidone ring can associate with noble metal. The association can prevent the noble metal NPs from aggregation. Au NPs have particular chemical properties, biocompatibility and unique electronic and optical properties [11-14]. Consequently, the incorporation of Au NPs into electrospun nanofibers is quite attractive for the development of functional composites. The interesting properties and the multi-functionality nature of these nanofibers are therefore quite applicable in fields as diverse as photonics, optoelectronics, biological medicine and catalysis [15-17].

In this paper, we synthesized Au NPs by using sodium citrate and tannic acid as the reduction agent. The PPV/PVP/Au composite nanofibers were successfully prepared by using the electrospinning technology. The microstructure, morphology and optoelectronic properties of the nanofibers were investigated, and we believed that the research would be useful for the study of other inorganic/organic composite nanomaterials.

2. EXPERIMENTAL

2.1 Materials

Tetrahydrothiophene and p-xylylene dichloride were purchased from Tokyo Chemical Industry Limited Company. Polyvinyl pyrrolidone (PVP, M.W.=1,300,000) was purchased from New Jersey (USA). $HAuCl_4$, sodium citrate, acetone and ethanol were all obtained from Sinopharm Chemical Reagent Co., Ltd. All the chemicals and solvents were used without further purification.

2.2 Preparation of Au NPs

Au NPs were synthesized by citric acid salt reduction method [18]. The synthesized Au NPs dispersion was centrifuged, washed repeatedly with distilled water and dispersed ultrasonically in water at last to form uniform solution. The Figure 1 showed that the size of the as-prepared Au NPs was ranged from 17 nm to 28 nm.
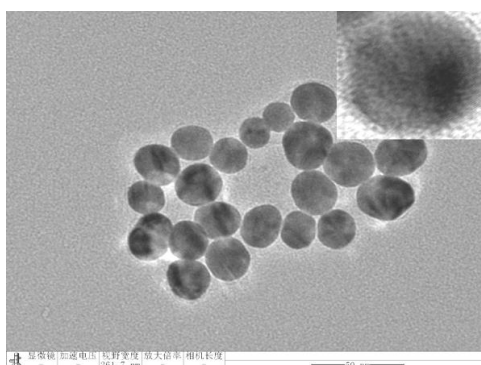
Figure 1. The TEM image of Au NPs.

2.3 Preparation of PPV Precursor

PPV precursor was prepared according to Wessling's synthetic route [19] and the optimized conditions provided by Halliday and co-workers [20]. Precursor aqueous solution was dialyzed in water for a week, and then it was placed in a ventilated place for a week to remove the water fully. As a result, the concentrated solution of PPV precursor was obtained.

2.4 Preparation of PPV/PVP/Au Precursor Solutions

0.2 g PVP was dissolved in 1.8 g ethanol to form 10% PVP solution. Then 3.0 g PPV precursor solution (the concentration of the solution was about 3 wt. %) was added to the PVP solution. The mixed solution was stirred for 10 min, and then Au NPs were added into the mixture. After stirring for a while, the solution became homogenous and it was ultrasonically treated for 10 min before electrospinning. The solutions were listed in Table 1.

Table 1. The PPV/PVP/Au NPs electrospun solutions.   Unit: g

NO.	PPV（3%）	PVP（10%）	Au NPs	PPV:PVP:Au NPs (Wt.)
PPA1	3.00	2.00	0.0029	9:20:0.29
PPA2	3.00	2.00	0.0058	9:20:0.58
PPA3	3.00	2.00	0.0116	9:20:1.16
PPA4	3.00	2.00	0.0174	9:20:1.74

2.5 Fabrication of the Composite PPV/PVP/Au Nanofibers

In this procedure, the PPV/PVP suspensions with different amounts of Au NPs were placed into a 10 mL syringe with a stainless steel needle (inner diameter=0.8 mm). Meanwhile, the anode was connected with the needle and the cathode with the aluminum foil, which was used as the nanofibers' collector. The feeding rate was kept constantly at 1.5 mL/h via a syringe pump. The applied voltage for electrospinning was 15 kV and the tip-to-collector distance was 20 cm. All the experiments were performed under room temperature.

2.6 Characterization

The surface morphology and size of the nanofibers was characterized by FE-SEM (MX2600FE). The samples for SEM analysis were spray-gold prior to observations. FEI-TEM (TECNAI F20) was used to study the internal morphology of the composite nanofibers, and investigations were performed on holey carbon-coated copper grids at an accelerating voltage of 200 kV. FT-IR spectra were recorded from a KBr window on a Nicolet AVATAR 360 FT-IR spectrophotometer. A combined stead state fluorescence and phosphorescence lifetime spectrometer

(FLSP920) was used to obtain the PL spectra of the as-spun nanofibers, and the excitation wavelength was 400 nm. The fluorescent images of nanofibers were taken from a fluorescence microscopy (TE2000-U). The crystallographic state of Au NPs and the phase composition of nanofibers were determined by X-ray diffraction (XRD). The photoelectric properties of the composite nanofibers were measured by electrochemical instrument (Bioanalytical Systems Inc. USA).

3. RESULTS AND DISCUSSION

3.1 Morphology Analysis
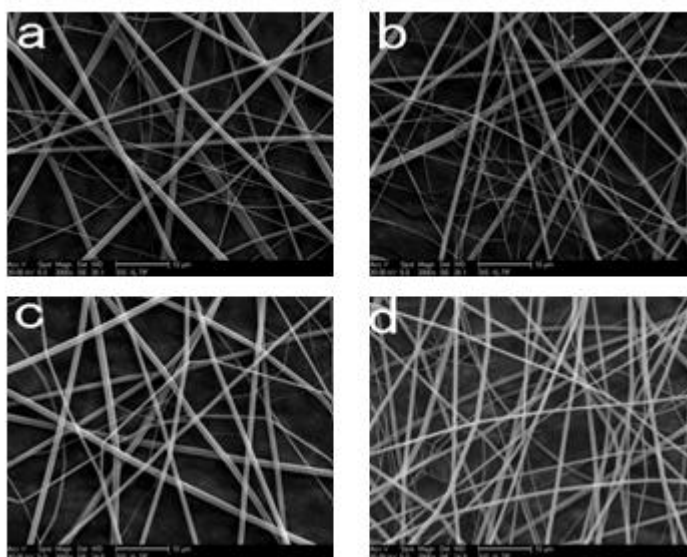
Figure 2. SEM images of (a) PPA1, (b) PPA2, (c) PPA3 and (d) PPA4 nanofibers.

Figure 2 showed the SEM images of the composite nanofibers. It was clearly seen that all the nanofibers were smooth and continuous. It was also shown that the average diameter of the composite nanofibers decreased from 583 nm (Figure 2a) to 415 nm (Figure 2d) with the increase of the Au NPs content in the electrospinning fibers. This phenomenon can be explained that the addition of Au NPs could increase the conductivity of the electrospinning solution, which had an important effect on the diameter of the composite nanofibers. It was reported that high conductivity resulted in sufficient elongation of a jet by electrical force, consequently produced thinner fibers [21].

The internal morphology and Au NPs dispersion of the composites were investigated by TEM, presented in Figure 3. It can be seen that the Au NPs were dispersed in the polymer matrix and remained their original size (about 21 nm). Some Au NPs aggregated because of the poor dispersion by ultrasound.
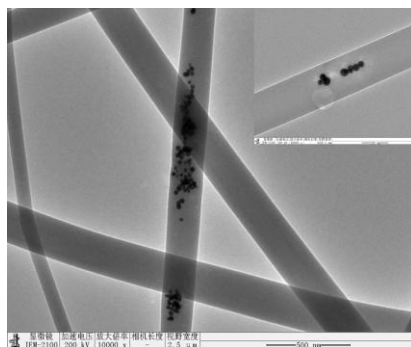
Figure 3. TEM image of PPA4 composite nanofibers.

3.2 FT-IR Spectra Analysis

Figure 4 presented the FT-IR spectra of the nanofibers in the wavenumber ranging from 500 to 2500 cm^{-1}. For the pure PPV nanofibers (Figure 4a), the absorption peak at 961 cm^{-1} was due to trans-vinylene δ(C-H) out-of-plane mode; the absorption peaks at 834 cm^{-1} and 1516 cm^{-1} were assigned to C-H plane bending vibration of p-substituted of benzene ring and C-C stretching vibration, which were in accordance with the report [22]. Figure 4b was the spectrum of the PPV/PVP composite nanofibers. The peaks at 1676 and 1422 cm^{-1} were assigned to C=O stretching vibration and C-N stretching vibration. For the PPV/PVP/Au composite nanofibers, the existence of Au didn't affect the peaks of PPV/PVP composites, and the curve looked the same to Figure 4b.
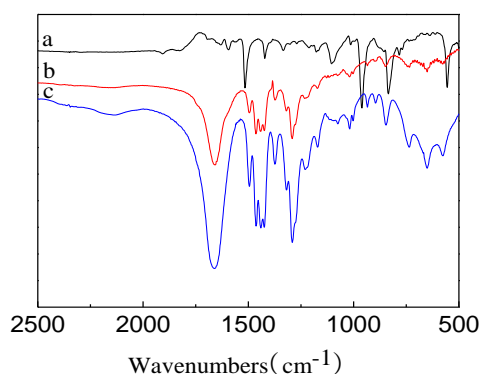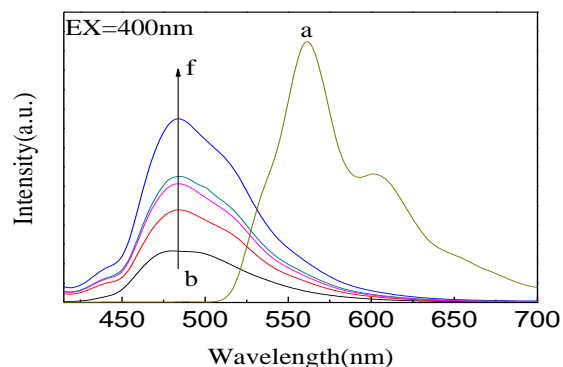

**Figure 4.** FT-IR spectra of (a) pure PPV, (b) PPV/PVP and (c) PPA4 nanofibers.

3.3 Fluorescence Spectra Analysis

In order to study the fluorescence characteristics of the nanofibers, the fluorescence spectra were obtained when the excitation wavelength was 400 nm. Pure PPV nanofibers had a main emission at 562 nm, shown in Figure 5a. The emission of PPV/PVP composite nanofibers was at 470 nm, which presented obvious blue shift compared with that of pure PPV. It is well known that the peak position of

PL spectra depends on the band gap of the π-π* transition, which is a function of the structure of PPV, and modifications with any specific purpose will affect the band gap and consequently the peak position. Therefore, the changes in the PL positions may be attributed to the interaction between C=C of the PPV chain and C=O of PVP, which interrupted the conjugation of PPV polymer chains and decreased the p-conjugated chain length [23, 24]. For the PPV/PVP/Au composite nanofibers, the main emission was almost unchanged with the increase of Au content, which was in accordance with the fluorescence photos in Figure 6.


Figure 5. Fluorescence emission spectra of (a) pure PPV nanofibers, (b) PPV/PVP composite nanofibers and (c-f) PPV/PVP/Au composite nanofibers (from PPA1 to PPA4).
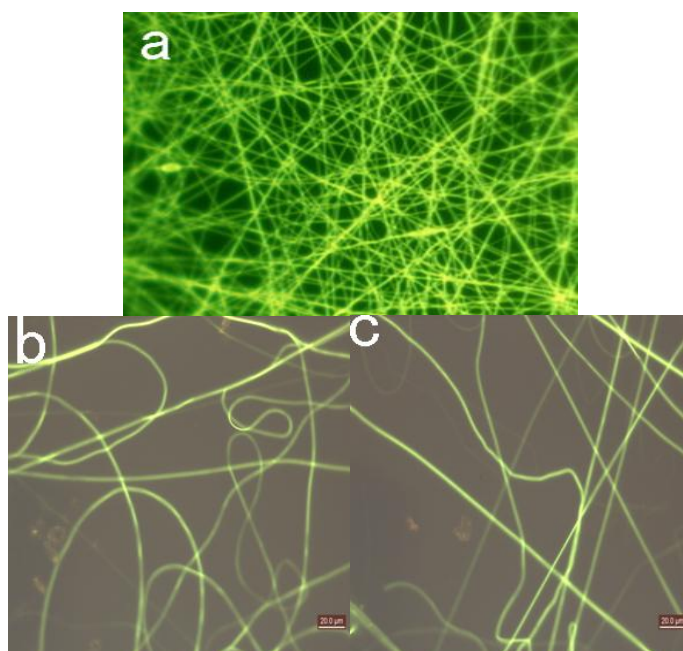
Figure 6. Fluorescence photos of nanofibers: (a) PPV, (b) PPV/PVP and (c) PPA4.

3.4 X-ray Diffraction Patterns

The crystalline phase evolution of the Au NPs and the resulting nanofibers has been examined using XRD measurements. In Figure 7, for the Au NPs, the diffraction peaks can be assigned to the diffraction planes of face-centred cubic according to the standard diffraction index. The peaks at 38.25°, 44.10°, 64.10° and 77.15° corresponded to the (111), (200), (220) and (311) crystal planes. Seen from the composite nanofibers, the polymer had a broad diffraction peak at 2θ=20.85°. Besides, the peaks of Au were also observed clearly, which indicated that the Au NPs still kept the original crystalline region even if it was incorporated into fibers.
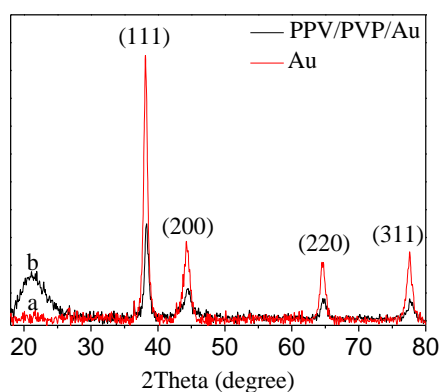
Figure 7. XRD patterns of (a) Au NPs and (b) PPA4 composite nanofibers.

3.5 Photoelectric Analysis
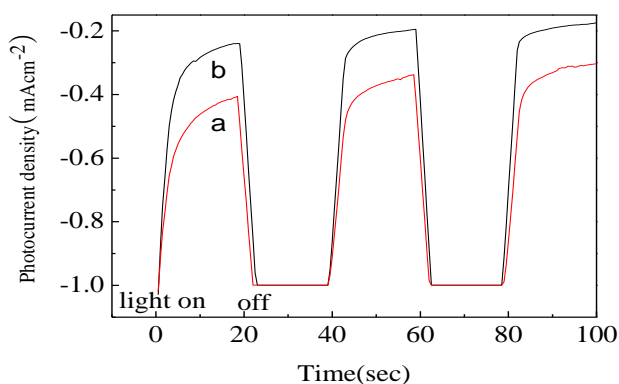
Figure 8. Photocurrent transient curves of the nanofibers: (a) PPV/PVP and (b) PPA4.

Figure 8 showed the photocurrent transient curves of the nanofibers array device. The light source was xenon lamp, and the applied voltage was -500 mV. Seen from the curves, the photocurrent density of the electrospun PPV/PVP/Au nanofibers (PPA4) was obviously stronger than that of

PPV/PVP nanofibers when light was on. For both the fiber samples, the notable photoresponse can be attributed to the rough surfaces of the electrospun nanofibers, which led to a high surface area-to-volume ratio, and subsequently resulted in many photogenerated carriers [25]. After compositing with Au, the photoelectric performance of the PPV/PVP nanofibers was further enhanced owing to the great conductivity of Au NPs.

4. CONCLUSION

In this study, PPV/PVP/Au composite nanofibers were successfully prepared by the electrospinning method. The as-prepared Au NPs with average diameter of 21 nm possessed the characters of face-centered cubic structure. The results from SEM and TEM images indicated that the average diameter of the resulting nanofibers decreased with the increase of Au NPs. In addition, the PL spectra and photos showed that the emission of PPV/PVP nanofibers presented obvious blue shift compared with pure PPV and the addition of Au NPs hardly affected the PL properties of fibers. This blue shift resulted from the decrease of PPV p-conjugated chain length, which was in accordance with the FT-IR analysis. The photocurrent transient curves of nanofibers showed that the addition of Au NPs could enhance the photoelectric performance of the composite nanofibers. The composite nanofibers should be a promising candidate for high-performance photodetector for many applications.

References

1. G.M. Odegard, T.C. Clancy and T.S. Gates, *Polymer*, 46 (2005) 553-560.
2. N. Hamizi, C. Ying and M. Johan, *Int. J. Electrochem. Sci.*, 7 (2012) 4727-4734.
3. X.F. Lu, D.M. Chao, J.Y. Chen, W.J. Zhang and Y. Wei, *Mater. Lett.*, 60 (2006) 2851-2854.
4. M.M. Sharif, P.S. Kumar, K.S.N. Murthy, S. Vijayanand and S. Ambalavanan, *Int. J. Electrochem. Sci.*, 6 (2011) 78-90.
5. W. Zhang, Z.H. Huang, E.Y. Yan, C. Wang, Y. Xin, Q. Zhao and Y.B. Tong, *Mater. Sci. Eng. A*, 443 (2007) 292-295.
6. A. Anis and S. M. Al-Zahrani, *Int. J. Electrochem. Sci.*, 7 (2012) 9161-9173.
7. Z.H. Huang, J.H. Yang, L.C. Chen, X.J Wang, W.L. Li, Y.Q. Qiu, J.T. Zhang and R.S. Wang, *Synthetic Met.*, 91 (1997) 315-319.
8. M. Lucero, M. Riquelme, G. Ramírez, M.C. Goya, A.G. Orive, A.H. Creus, M.C. Arévalo and M.J. Aguirre, *Int. J. Electrochem. Sci.*, 7 (2012) 222-233.
9. G.Q. Zhang, X. Li, H.T. Jia, X.X. Pang, H.W. Yang, Y.H. Wang and K.Q. Ding, *Int. J. Electrochem. Sci.*, 7 (2012) 819-829.
10. A.R. Brown, N.C. Greenham, J.H. Burroughes, D.D.C. Bradley and R.H. Friend, *Chem. Phys. Lett.*, 200 (1992) 46-54.

11. H.H. Huang, X.P. Ni, G.L. Loy, C.H. Chew, K.L. Tan, F.C. Loh, J.F. Deng and G.Q. Xu, *Langmuir*, 12 (1996) 909-912.
12. S.Y. Li, W.H. Ma, Y. Zhou, X.H. Chen, M.Y. Ma, Y.H. Xu, Z. Ding and X.H. Wu, *Int. J. Electrochem. Sci.*, 8 (2013) 1794-1801.
13. B.S. Yin, H.Y. Ma, S.Y. Wang and S.H. Chen, *J. Phys. Chem. B*, 107 (2003) 8898-8904.
14. X.H. Tu, L. Chen, J.F. Shen, Y. Zhang, C.P. Miao and J.Y. Wu, *Int. J. Electrochem. Sci.*, 7 (2012) 9560-9572.
15. J. Bai, Y.X. Li, J.S. Du, S.G. Wang, J.F. Zheng, Q.B. Yang and X.S. Chen, *Mater. Chem. Phys.*, 106 (2007) 412-415.
16. J. Bai, Y.X. Li, S.T. Yang, J.S. Du, S.G. Wang, J.F Zheng, Y.Z. Wang, Q.B. Yang, X.S. Chen and X.B. Jing, *Solid State Commun.*, 141 (2007) 292-295.
17. R.M. Piasentin, R.F.B. Souza, J.C.M. Silva, E.V. Spinacé, M.C. Santos and A.O. Neto, *Int. J. Electrochem. Sci.*, 8 (2013) 421-434.
18. C.Y. Tsai, H.T. Chien, P.P. Ding, B. Chan, T.Y. Luh and P.H. Chen, *Mater. Lett.*, 2004, 58 (9): 1461-1465.
19. R.A. Wessling, *J. Polym. Sci: Pol. Symp.*, 72 (1985) 55-66.
20. D.A.D. Halliday, P.L. Burn, R.H. Friend, D.D.C. Bradley and A.B. Holmes, *Synthetic Met.*, 55 (1993) 902-907.
21. M.I. Baraton, L. Merhari, J.Z. Wang and K.E. Gonsalves, *Nanotechnology*, 9 (1998) 356-359.
22. Y. Xin, Z. H. Huang, C.J. Feng, C. Wang, Y.B. Tong and S.D. Liu, *Mater. Lett.*, 62 (2008) 991-993.
23. K. Kim, S.C. Jeoung, J. Lee, T. Hyeon and J.I. Jin, *Macromol. Symp.*, 201 (2003) 119-126.
24. D. Li, A. Babel, S.A. Jenekhe and Y.N. Xia, *Adv. Mater.*, 16 (2004) 2062-2066.
25. Y. Xin, Z.H. Huang, L. Peng and D.J. Wang, *J. Appl. Phys.*, 105 (2009) 086106.